2011 American Control Conference
on O'Farrell Street, San Francisco, CA, USA
June 29 - July 01, 2011

Effect of Coupling Point Selection on Distortion in Internet-distributed Hardware-in-the-Loop Simulation

Tulga Ersal, R. Brent Gillespie, *Member, IEEE*, Mark Brudnak, *Member, IEEE*, Jeffrey L. Stein, and Hosam K. Fathy

***Abstract*—Internet-distributed hardware-in-the-loop (ID-HIL) simulation integrates HIL setups between geographically dispersed engineering teams and fosters concurrent systems testing early in the design process. The question naturally arises: what is the cost in fidelity incurred by distributing the simulation across Internet links? The degree to which an Internet-distributed simulation loses fidelity relative to a single-location HIL setup is referred to as *distortion* in this paper. Various factors affect distortion, including the Internet's delay, jitter, and loss, as studied extensively in the literature. Additional considerations, however, such as the coupling points, i.e., the particular points at which the system model shall be divided to enable distribution across the Internet, also affect distortion. The aim of this paper is to turn coupling point selection into a design decision that can be used to minimize distortion. To quantify distortion, a frequency-domain metric is proposed using a linear systems framework. This metric is then used to analyze how the choice of the coupling point affects distortion, and it is also linked to a sensitivity function, which is easier to interpret physically. This analysis can be used in an ID-HIL setup to pick a coupling point that gives minimal distortion, and is the first step towards analyzing the trade-off between stability robustness and transparency in an ID-HIL system.**

I. INTRODUCTION

HARDWARE-IN-THE-LOOP simulation (HILS) refers to simulating a system by coupling the physical models of some of its components together with the mathematical models of its remaining components [1]. Thus, it combines the high fidelity of physical prototyping with the cost effectiveness of model-based simulation [2]. It strongly promotes concurrent system engineering and has therefore become indispensable in many application areas, such as automotive [3, 4], aerospace [5, 6], manufacturing [7], robotics [8, 9], and defense [10, 11].

To fully exploit the benefits of HILS, it may be desirable to integrate multiple HILS setups [12]. Recent efforts have focused on achieving such integration over the Internet to allow for integration of setups that are geographically dispersed and unfeasible to couple physically. For example, the George E. Brown Jr. Network for Earthquake Engineering Simulation (NEES) [13] provides an outstanding example of the capabilities and impact of the ID-HILS idea, and the earthquake literature presents many other applications of the ID-HILS idea to earthquake simulation [14-19]. Another example is the integration of a ride motion simulator in Warren, MI, USA, with a hybrid-powertrain-system simulator in Santa Clara, CA, USA [20-22] and, as a separate work, with an engine-in-the-loop simulator in Ann Arbor, MI, USA [23].

Coupling HILS setups over the Internet introduces a deviation from the dynamics that would otherwise be observed if the setups were collocated and could be directly integrated. This deviation is termed *distortion* in this paper.

There are several sources of distortion in an ID-HIL setup. Distributing a system into subsystems that are co-simulated using independent numerical solvers can be in and of itself an important source of distortion due to the lack of access to the Jacobians of the remote sites, sampling effects, etc., even without any delay [24]. Distribution over the Internet introduces further distortion due to the Internet's delay, jitter, and loss. Recognizing these issues, the literature proposed methods to assess the relative impact of distribution effects in comparison to the effects of the Internet's delay, jitter, and loss [24]. The literature also developed various approaches, e.g., passivity-based [25-28], event-based [19, 29, 30], and observer-based [20-22] frameworks, to address stability and distortion issues under a delayed coupling of subsystems.

This paper focuses on another potential variable that can affect distortion, namely, the coupling point. Within the context of this paper, coupling point refers to the point at which the HILS system is divided into two subsystems that are then co-simulated. While options for placement of the coupling point may not always exist, when they do exit, the location of the coupling point can become a design parameter. Then, it becomes important to know how to best choose that design parameter to minimize distortion.

Thus, the aim of this paper is to develop a framework in which the impact of coupling point selection on distortion can be studied and the reasons that make one coupling point better than another can be understood. As a first step, this paper will consider only the delay, and ignore the jitter, loss, and the effects of decentralized solvers. This will not only simplify the problem, but also allow for the analysis to be handled through a linear framework. A linear framework will, in turn, allow for leveraging the existing frequency-

Manuscript received September 22, 2010. This work was supported by the Automotive Research Center at the University of Michigan.

T. Ersal, R. B. Gillespie, and Jeffrey L. Stein are with the Department of Mechanical Engineering, University of Michigan, Ann Arbor, MI 48109 USA. (e-mail: {tersal, brentg, stein}@umich.edu).

M. Brudnak is with the U.S. Army RDECOM-TARDEC, Warren, MI 48397 USA. (e-mail: mark.brudnak@us.army.mil).

H. K. Fathy (corresponding author) is with the Pennsylvania State University, University Park, PA 16802 USA. (e-mail: hfk2@psu.edu).

domain characterizations of distortion [31-35].

The rest of the paper is organized as follows. A motivating example is given first in Section II that illustrates how the location of the coupling point can affect distortion. Then, in Section III.A, a frequency-domain distortion metric from the haptics literature is adopted into the ID-HIL framework. Using this metric, Section III.B investigates which coupling point characteristics lead to a low distortion, and relates distortion to a sensitivity function. Section III.C establishes the signal-dependence of distortion, Section III.D discusses the effect of causality on distortion, and Section III.E analyzes if the existence of a subsequent feedback control design problem affects how the coupling point should be chosen. Finally, in Section IV, the theory developed is applied to the illustrative example, and conclusions are drawn in Section V.

II. Motivating Example

Consider the system shown in Fig. 1. The figure also shows the two coupling point candidates considered in this study, labeled as CP1 and CP2. A constant time delay of τ is considered in both directions of communication, leading to a round-trip time delay of 2τ. The input is the force F applied to the mass m_1, and the output of interest is the displacement x_1 of mass m_1. The parameter values of the system are given in Table I.

Fig. 2 compares the unit step responses of the ideal system and the two systems in which the coupling variables

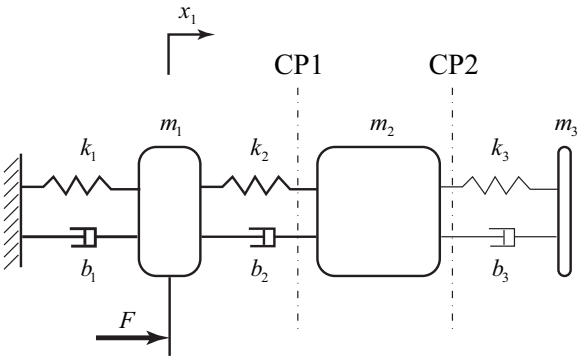

Fig. 1.Example system with two locations as potential coupling points

TABLE I
PARAMETERS OF THE EXAMPLE SYSTEM

Parameter	Value
b_1	0.3 Ns/m
b_2	0.1 Ns/m
b_3	0.01 Ns/m
k_1	1 N/m
k_2	1 N/m
k_3	0.1 N/m
m_1	5 kg
m_2	10 kg
m_3	0.1 kg
τ	0.1 s

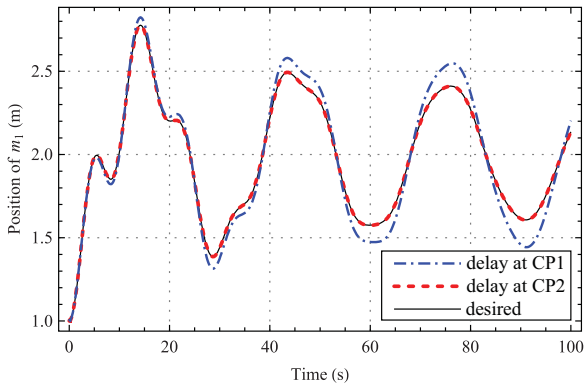

Fig. 2.Comparing the unit steps responses of the ideal system and the two systems with delays at CP1 and CP2

force and velocity at CP1 and CP2 are communicated with the constant time delay of τ. As seen in the figure, a delay at CP1 causes much more distortion than a delay at CP2. This exemplifies the impact of the location of the coupling point on distortion.

III. Coupling Point Analysis

A. A Metric for Distortion

In this paper, distortion is a transfer function that is defined as the difference between the reference dynamics R_d and actual dynamics P, where R_d represents the dynamics of a HIL setup that is not distributed and P represents the dynamics of the same HIL setup with delay inserted at the coupling point, representing distribution across the Internet. It is also useful to normalize distortion by the reference dynamics R_d, yielding the following:

$$\Theta = \frac{P - R_d}{R_d} \tag{1}$$

This definition of distortion was first introduced by Griffiths et al. within the haptics domain, where R_d represented the dynamics desired to be rendered to the user through the haptic device, and P represented the actual dynamics rendered to the user [35].

In the following, an ID-HIL system is treated involving only two sites, called local and remote. The reference dynamics R_d in this case are achieved through an ideal coupling (involving bilateral communications without delay) of the local and remote dynamics. Fig. 3 depicts the reference dynamics in block diagram form, where G and G_r refer to the local and remote dynamics, respectively, u_1 is the external input to the local system, y_1 is the output of interest in the local system, and u_2 and y_2 are the coupling variables between the local and remote systems. Generally, the variables u_2 and y_2 are power-conjugate variables modeling an energetic connection, such as force and velocity in the mechanical domain, but this need not be true in every ID-HIL system. The desired system equations are given as

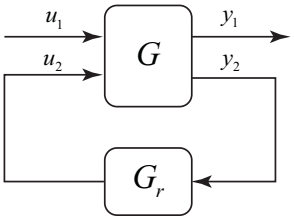

Fig. 3. Expressing the desired dynamics in block diagram form

$$\begin{bmatrix} y_1 \\ y_2 \end{bmatrix} = \begin{bmatrix} G_{11} & G_{12} \\ G_{21} & G_{22} \end{bmatrix} \begin{bmatrix} u_1 \\ u_2 \end{bmatrix} \qquad (2)$$
$$u_2 = G_r y_2$$

from which the desired dynamics, R_d, from u_1 to y_1 can be derived as

$$R_d = \frac{G_{11} + \left(G_{12}G_{21} - G_{11}G_{22}\right)G_r}{1 - G_{22}G_r} = \frac{G_{11} + A}{1 - G_{22}G_r} \qquad (3)$$

where $A = \left(G_{12}G_{21} - G_{11}G_{22}\right)G_r$. Making the coupling point explicit enables an analysis of the effects of choosing different coupling points.

Next, to capture the effect of introducing Internet communications in an ID-HIL setup, consider a multiplicative perturbation, Δ, to the remote dynamics, G_r. This multiplicative form is suitable for capturing the dynamics of Internet delay, and could also capture other unmodeled dynamics such as the dynamics of the sensors and actuators. Then, Fig. 4 expresses the adoption of the distortion metric into the ID-HIL framework in block diagram form, where distortion is the transfer function from u_1 to d.

The actual system equations become

$$\begin{bmatrix} \tilde{y}_1 \\ \tilde{y}_2 \end{bmatrix} = \begin{bmatrix} G_{11} & G_{12} \\ G_{21} & G_{22} \end{bmatrix} \begin{bmatrix} u_1 \\ \tilde{u}_2 \end{bmatrix} \qquad (4)$$
$$\tilde{u}_2 = \Delta G_r \tilde{y}_2$$

where tildes are used to differentiate the ideal variables from the actual variables. From Eq. (4), the actual dynamics P from u_1 to $\tilde{y}_1$ can be derived as

$$P = \frac{G_{11} + \Delta A}{1 - \Delta G_{22}G_r} \qquad (5)$$

The distortion metric for the ID-HIL framework can then be found as

$$\Theta = \frac{P - R_d}{R_d} = \frac{G_{12}G_{21}G_r\left(\Delta - 1\right)}{\left(1 - \Delta G_{22}G_r\right)\left(G_{11} + A\right)} \qquad (6)$$

Eq. (6) provides a means to analyze the impact on distortion of different coupling points in an ID-HIL system. Different coupling points will lead to different definitions of local and remote dynamics, i.e., different G_{11}, G_{12}, G_{21}, G_{22}, and G_r, even though the delay dynamics and other perturbation factors lumped in Δ may remain invariant, which is assumed to be the case in this paper. Therefore, different coupling points will, in general, yield different distortion values, and Eq. (6) can quantify their impact on distortion.

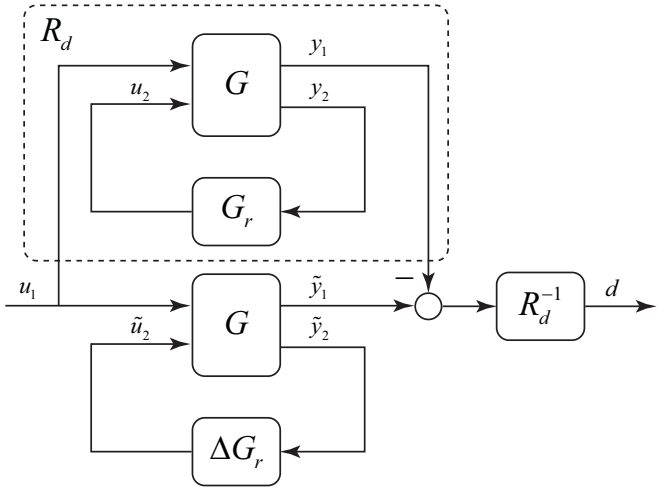

Fig. 4. Adoption of the distortion metric into the ID-HIL framework

B. Distortion Analysis

In the framework created in section III.A, the ultimate goal of bringing the actual dynamics as close to the desired dynamics as possible translates to achieving a distortion that is as small as possible. Since distortion is a transfer function and thus a function of frequency, it is also possible to define frequency ranges over which the distortion is desired to be small.

Eq. (6) reveals that there are a number of ways to achieve a small distortion at a given frequency. Specifically, besides the trivial case of $\Delta \equiv 1$, i.e., no perturbation, the distortion will be small for a given frequency, if one of the following is true at that frequency:

1. $G_{11} \to \infty$: the input u_1 is greatly amplified at the output y_1 and thus the contribution through the coupling with the remote system is negligible.
2. $G_{12} \to 0$: the feedback u_2 from the remote system has a very small effect on the output of interest y_1.
3. $G_{21} \to 0$: the external input u_1 has a very small effect on the coupling variable y_2.
4. $G_r \to 0$: the remote system does not affect the local system, i.e., it is driven by the local system without any impedance and the coupling is almost one-way.
5. $G_r \to \infty$: the remote system is acting almost like a wall, resisting even the smallest input y_2.
6. $G_{22} \to \infty$: the local impedance at the coupling point is so high that the local system is acting almost like a wall to the remote system.

Thus, to achieve low distortion, one should look for a coupling point that will lead to one of the conditions listed above. The physical interpretation associated with each condition can help in making the assessments by inspection. However, it is not realistic to expect that one of these

conditions would be satisfied perfectly. In that case, it will be necessary to consider all the conditions simultaneously when comparing coupling points, which may make it difficult to utilize physical insight. Nevertheless, although the conditions above may seem unrelated at first sight, there actually exists a concept that unifies them all, and that concept is the sensitivity of the desired dynamics to the remote dynamics. A formal definition is given by

$$S_r \triangleq \frac{\partial R_d / R_d}{\partial G_r / G_r} \tag{7}$$

In words, it is defined as the ratio of a relative change in the desired dynamics to a relative change in the remote dynamics. Evaluation of S_r for the framework given in Fig. 3 leads to

$$S_r = \frac{G_{12}G_{21}G_r}{\left(1-G_{22}G_r\right)\left(G_{11}+A\right)} \tag{8}$$

Comparing Eq. (6) and (8), the following relationship between distortion and sensitivity to remote dynamics can be derived:

$$\Theta = S_r \frac{1-G_{22}G_r}{1-\Delta G_{22}G_r}\left(\Delta-1\right) \tag{9}$$

From Eq. (9) it can be seen that distortion will be small when the sensitivity to remote dynamics is small, and it can be easily verified that the conditions listed previously are also the conditions under which S_r becomes small. Hence, S_r provides a unifying concept for those conditions and also a single intuitive, physical explanation for distortion. Also, this sensitivity function may be more easily generalized to nonlinear systems than the distortion metric.

Furthermore, expanding the expression for distortion in Eq. (6) in a Taylor series around $\Delta = 1$ shows that, to a first order approximation, distortion is given by $S_r\left(\Delta-1\right)$, i.e.,

$$\Theta = S_r\left(\Delta-1\right) + O\left(\left(\Delta-1\right)^2\right) \tag{10}$$

Thus, to a first order approximation, and recalling that Δ is assumed to be invariant to the location of the coupling point, the difference in distortions caused by different coupling points is completely captured by the sensitivity function S_r. The significance of this finding can be seen by referring to Eq. (8) and noting that S_r can be evaluated without the knowledge of the perturbation Δ. Therefore, S_r not only provides a single metric to be considered when comparing coupling points, but also this metric is, unlike Θ itself, independent of Δ. This allows for comparing coupling points without having to derive an expression for Δ.

Eq. (10) further implies that

$$S_r = \frac{\partial R_d / R_d}{\partial G_r / G_r} = \left.\frac{\partial \Theta}{\partial \Delta}\right|_{\Delta=1} \tag{11}$$

That is, the sensitivity S_r is the gradient of the distortion metric with respect to the perturbation Δ at $\Delta = 1$, i.e., the case when there is no perturbation.

Having related S_r to Θ, we can now go back to Eq. (7) to explain how a coupling point can be selected. Distortion will be small if a relative change in the remote dynamics creates a small relative change in the desired dynamics. Thus, the task of finding the best coupling point now translates to finding the coupling point that partitions into G_r all the dynamics whose relative change affects the desired system dynamics the least.

C. On the Signal Dependence of Distortion

It is important to note that distortion is defined for a particular output of interest y_1. Even though the formulation allows y_1 to be any signal in the local system, a low distortion in y_1 does not necessarily imply that the distortion will be low in *all* signals in the local system. This is easily demonstrated by considering the distortions in y_1 and y_2 simultaneously.

Following the same steps as for y_1, the distortion in y_2 can be derived as

$$\Theta_{y_2} = \frac{G_{22}G_r\left(\Delta-1\right)}{1-\Delta G_{22}G_r} \tag{12}$$

Thus, it can be seen that, besides the trivial condition $\Delta \to 1$, there is only one condition under which both Θ and Θ_{y_2} become small, namely, $G_r \to 0$. The conditions 1, 2, 3, 5, and 6 do not necessarily imply a small Θ_{y_2}, and the condition $G_{22} \to 0$, which makes Θ_{y_2} small, does not necessarily make Θ small. This emphasizes the fact that distortion is not a property of the system, but is output-signal dependent. Therefore, when considering a distortion analysis, it is important to keep the signals in mind with respect to which distortion was defined.

D. On the Effect of Causality on Distortion

Under some conditions, distortion can be improved simply by changing the causality. Consider the case when $G_{22} \to 0$. Furthermore, assume that G_{22}^{-1} and G_r^{-1} are proper. In this case, a switch in causality as shown in Fig. 5 leads to the following ideal system equations

$$\begin{bmatrix} y_1 \\ u_2 \end{bmatrix} = \begin{bmatrix} G_{11} & G_{12}G_{22}^{-1} \\ -G_{21}G_{22}^{-1} & G_{22}^{-1} \end{bmatrix} \begin{bmatrix} u_1 \\ y_2 \end{bmatrix} \tag{13}$$
$$y_2 = G_r^{-1}u_2$$

which gives

$$R_d^* = \frac{G_{12}G_{21} + G_{11}G_{22}\left(1-G_{22}G_r\right)}{G_{22}\left(1-G_{22}G_r\right)} \tag{14}$$

where the asterisk is used to denote the switched-causality case. Assuming a multiplicative perturbation Δ as before leads to

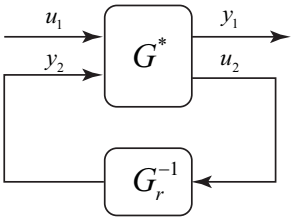

Fig. 5. Switching causality at the coupling point

$$P^* = \frac{\Delta G_{12}G_{21} + G_{11}G_{22}\left(\Delta - G_{22}G_r\right)}{G_{22}\left(\Delta - G_{22}G_r\right)} \tag{15}$$

Finally, the expression for distortion is obtained as

$$\begin{aligned}\Theta^* &= \frac{P^* - R_d^*}{R_d^*} \\ &= \frac{(1-\Delta)G_{12}G_{21}G_{22}G_r}{\left(\Delta - G_{22}G_r\right)\left(G_{12}G_{21} + G_{11}G_{22}\left(1 - G_{22}G_r\right)\right)}\end{aligned} \tag{16}$$

From Eq. (16) it can be seen that

$$\lim_{G_{22}\to 0} \Theta^* = 0 \tag{17}$$

Thus, distortion is reduced by switching the causality at the coupling point. Note that, in practice, such switching may require filters to ensure proper transfer functions.

E. On Distortion Compensation through Feedback Control

The distortion analysis presented in section III.B suggests that the coupling point that gives the minimum distortion is the one that leads to the smallest sensitivity of the desired dynamics to the remote system. However, it is easy to conceive of a case in which the lowest distortion that can be achieved through coupling point selection is still not low enough. In this case, further attenuation of distortion through feedback control may be considered. This can lead to a general control configuration as shown in Fig 6. This is only one of the possible feedback configurations which present a fundamental trade-off that is worth a discussion, because it may have an effect on the selection of the coupling point.

As shown by Freudenberg et al. [36] first and Griffiths et al. [35] later, this general control configuration presents a trade-off between distortion attenuation and closed-loop sensitivity, which is an indicator for stability robustness. This trade-off is formally expressed as

$$\frac{\Theta_{cl}}{\Theta} = 1 + \Gamma\left(S - 1\right) \tag{18}$$

where

$$\Theta_{cl} = \frac{1}{R_d}\left(\frac{P}{1 - PK} - R_d\right) \tag{19}$$

is the closed-loop distortion,

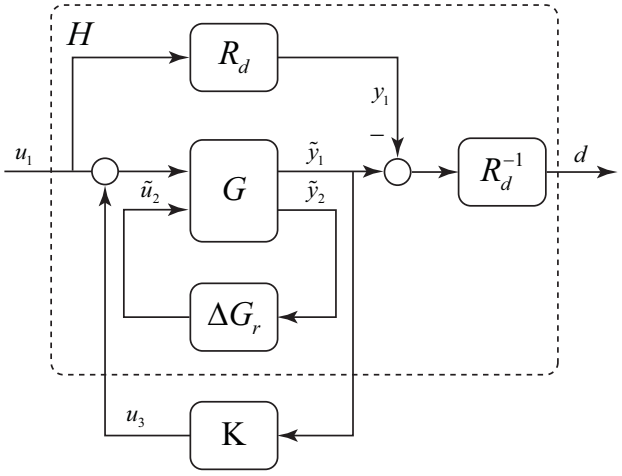

Fig. 6. Expressing feedback control to attenuate distortion as a general control configuration

$$S = \frac{1}{1 - PK} \tag{20}$$

is the sensitivity function of the closed-loop, and

$$\Gamma = \frac{H_{12}H_{21}}{H_{11}H_{22}} \tag{21}$$

is the trade-off severity, and H is the multivariable open-loop system.

From Eq (18) it can be seen that if $\Gamma = 1$, then the relative distortion, i.e., the ratio of closed-loop distortion to open-loop distortion, is completely described by the sensitivity function, meaning that closed-loop distortion and sensitivity can be attenuated simultaneously, i.e., there is no trade-off. If, however, $\Gamma \neq 1$, then there exists a trade-off between relative distortion and sensitivity, as they cannot be attenuated simultaneously.

For the particular control architecture given in Fig 6, we have

$$\begin{aligned}H_{11} &= \Theta \\ H_{12} &= \Theta + 1 \\ H_{21} &= H_{22} = P\end{aligned} \tag{22}$$

which leads to the following relationship between the trade-off severity and the open-loop distortion:

$$\Gamma = 1 + \frac{1}{\Theta} \tag{23}$$

This, then, brings up an important question: How does this fundamental trade-off affect the coupling point selection strategy?

To answer that question, the trade-off equation (18) needs to be investigated in more detail. Specifically, consider the limiting case of perfect closed-loop distortion attenuation and its cost in terms of sensitivity. This can be done by setting Eq. (18) equal to zero, and solving for S:

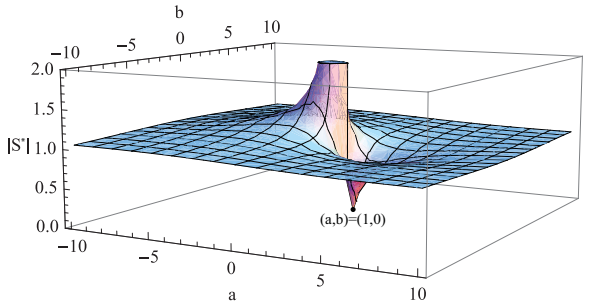

Fig. 7. The relationship between trade-off severity and magnitude of closed-loop sensitivity for the case of perfect closed-loop distortion attenuation

$$S^* = 1 - \frac{1}{\Gamma} \tag{24}$$

where the asterisk is used to differentiate this limiting case from the general case. Noting that Γ is a complex variable, i.e., $\Gamma = a + bi$, the magnitude of S^* can be plotted against the components a and b of Γ as shown in Fig. 7.

Fig. 7 explicitly reveals that the magnitude of sensitivity for zero relative distortion quickly saturates to 1 as Γ increases. The region where the magnitude of sensitivity is either very low or very large is quite narrow, and outside that region the magnitude of sensitivity is close to 1 regardless of the trade-off severity Γ. Therefore, if the open-loop distortion is small enough for all coupling points in consideration to ensure that Γ is outside that region, then the fundamental trade-off is not a major decision factor, since closed-loop sensitivity will be close to 1 for all coupling points.

The other interesting case is that if there is a coupling point that makes the open-loop distortion very high. In that case Γ will be close to 1, and there will hardly be a significant trade-off between relative distortion attenuation and closed-loop sensitivity. Note, however, that the region in which the trade-off is small is very narrow, and the sensitivity can increase very quickly in the close neighborhood of $\Gamma = 1$. This means that the low trade-off case may not be very robust, and care must be exercised when choosing a coupling point with very high open-loop distortion for the purposes of reducing the fundamental trade-off in the subsequent feedback design.

IV. Application to the Simple Example

In this section, the theory that is presented in Section III is applied to the simple system introduced in Section II for illustration purposes.

An analysis of distortion using the proposed framework provides a frequency domain explanation into the different levels of performance observed with the two coupling points for the same delay conditions. Fig. 8 compares the distortion metric for the two coupling points. As the figure clearly shows, the distortion for the system with CP2 is much lower than the distortion for the system with CP1 at all

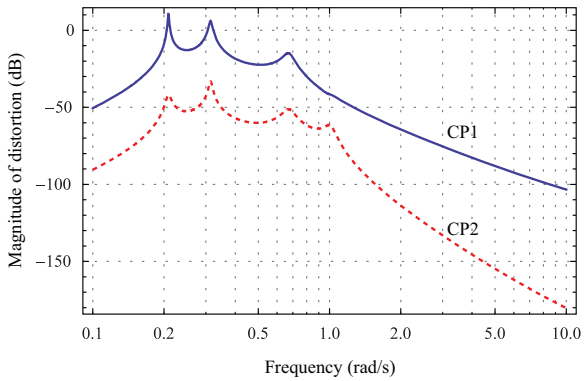

Fig. 8. The magnitude of the distortion metric for the two coupling points CP1 and CP2

frequencies, and hence, CP2 is a better choice of coupling point than CP1.

To gain more physical insight, Fig. 9 compares the sensitivity, S_r, of the desired dynamics to the remote dynamics for the two coupling points CP1 and CP2. The sensitivity S_r is less for CP2 than CP1, explaining why the distortion with CP2 is lower relative to the distortion with CP1. Specifically, CP1 partitions the largest mass m_2 into the remote system G_r. It is easy to see intuitively that a relative change in m_2 would affect the system dynamics more than the same relative change in m_3, for example. Hence, CP2, which considers as G_r only the mass-spring-damper system m_3, k_3, b_3, which has only a small effect on the system dynamics, is a better choice than CP1.

Fig. 10 further reveals more in detail why the sensitivity S_r, and thus distortion, is low for CP2. Specifically, the distortion is low due to small G_r for frequencies up to approximately 0.8 rad/s. That is, the local system affects the remote system dynamics but is not affected by them itself due to the relatively small reaction forces generated by the remote system with the relatively small mass m_3. In higher frequencies, however, the small G_{12} is the dominating reason for a small distortion. This means that, in this frequency range, the distortion is small because the reaction force of the remote system cannot affect the output of interest significantly due to the small bandwidth of the local system. The transfer functions G_{11}, G_{21}, and G_{22} are not

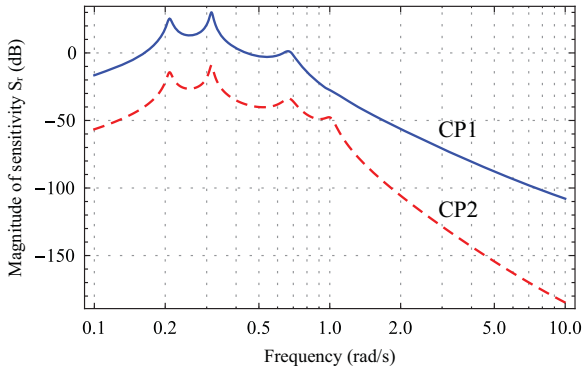

Fig. 9. The magnitude of sensitivity of the desired dynamics to the remote dynamics for the two coupling points CP1 and CP2

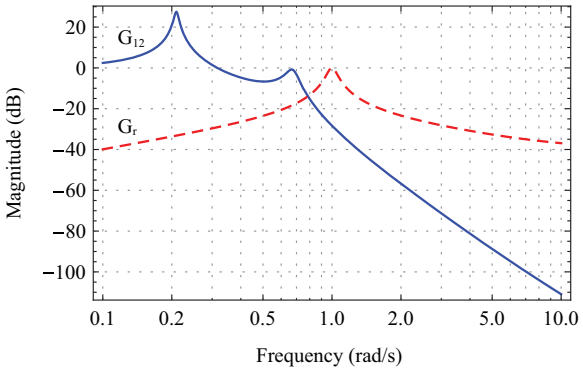

Fig. 10. The magnitude of G_{12} and G_r for CP2 as dominating factors leading to a low sensitivity S_r

shown in Fig. 10, because they are dominated by either G_r or G_{12} depending on the frequency.

Finally, Fig. 11 shows the trade-off severity for a perfect closed-loop distortion attenuation. The trade-off severity is large enough for both coupling points such that their closed-loop sensitivities are around the saturation level of 1 for most frequencies as seen in Fig. 12. Thus, the trade-off between relative distortion and sensitivity does not seem to significantly affect the coupling point selection in this example.

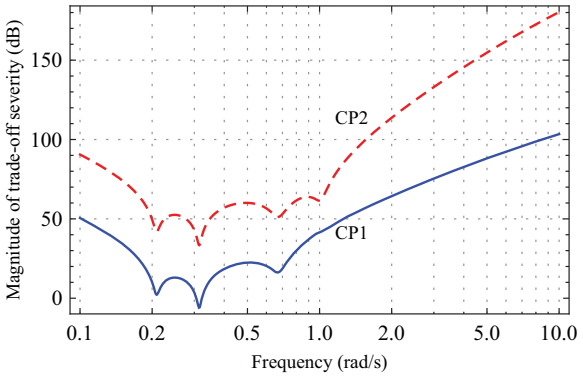

Fig. 11. The magnitude of trade-off severity Γ for CP1 and CP2

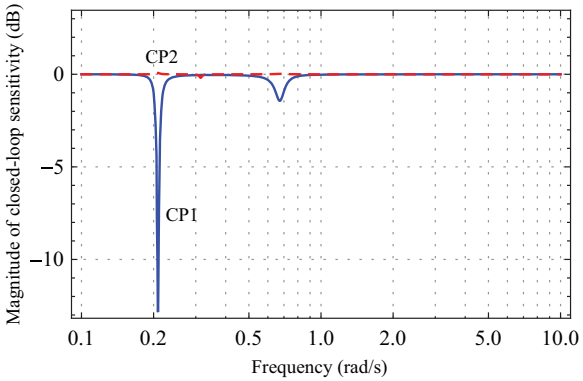

Fig. 12. The magnitude of closed-loop sensitivity S for the case of perfect closed-loop distortion attenuation

V. Conclusion

The original contributions of this paper can be summarized as follows. This paper considers the coupling point as a design variable in ID-HILS systems and proposes a framework for a frequency-domain analysis of the impact of the location of the coupling point to distortion. Using this framework, the paper identifies the sensitivity of the desired dynamics to the dynamics of the remote system as the unifying reason for different distortion results obtained with different coupling points. It also shows that distortion is an output-signal dependent concept and can, in some cases, also be affected not only by the location of the coupling point, but also by the coupling causality. Finally, the paper shows that coupling point selection may not be affected by the existence of a subsequent feedback control design problem and the trade-off severity concept associated with it, when the open-loop distortion is below a certain threshold for all coupling point candidates.

The framework used in this paper relies on the following assumptions: linearity, SISO remote system, and invariance of the multiplicative uncertainty to the coupling points. In general, ID-HILS systems can involve nonlinear, multivariable systems, and different coupling points can require different sensors and actuators that may significantly change the multiplicative uncertainty. The interested reader is referred to the references [23, 24] for an example ID-HILS setup. Thus, while the results presented in this paper are useful to gain insight into the coupling point selection problem, it is highly desirable to extend these results to nonlinear, multivariable ID-HILS systems, which will be the focus of future work. It is also desired to generalize the results to the coupling of more than two subsystems.

Finally, even though this paper focuses on minimization of distortion, it is also important to note that there may be other factors that affect the coupling point selection, such as availability of models, load distribution, safety, intellectual property, and cost.

References

[1] M. Bacic, S. Neild, and P. Gawthrop, "Introduction to the special issue on hardware-in-the-loop simulation," *Mechatronics*, vol. 19, no. 7, pp. 1041-1042, 2009.

[2] H. K. Fathy, Z. S. Filipi, J. Hagena, and J. L. Stein, "Review of hardware-in-the-loop simulation and its prospects in the automotive area," SPIE - Modeling and Simulation for Military Applications, Kissimmee, FL, United States, vol. 6228, pp. 1-20, SPIE, 2006.

[3] A. Kimura and I. Maeda, "Development of engine control system using real time simulator," 1996 IEEE International Symposium on Computer-Aided Control System Design, pp. 157-163, 1996.

[4] R. Verma, D. Del Vecchio, and H. K. Fathy, "Development of a scaled vehicle with longitudinal dynamics of an HMMWV for an ITS testbed," *IEEE/ASME Transactions on Mechatronics*, vol. 13, no. 1, pp. 46-57, 2008.

[5] J. Leitner, "A hardware-in-the-loop testbed for spacecraft formation flying applications," 2001 IEEE Aerospace Conference, vol. 2, pp. 615-620, IEEE, 2001.

[6] X. Yue, D. M. Vilathgamuwa, and K.-J. Tseng, "Robust adaptive control of a three-axis motion simulator with state observers," *IEEE/ASME Transactions on Mechatronics*, vol. 10, no. 4, pp. 437-448, 2005.

[7] A. Ganguli, A. Deraemaeker, M. Horodinca, and A. Preumont, "Active damping of chatter in machine tools - demonstration with a 'hardware-in-the-loop' simulator," *Journal of Systems and Control Engineering*, vol. 219, no. 5, pp. 359-369, 2005.

[8] F. Aghili and J.-C. Piedboeuf, "Contact dynamics emulation for hardware-in-loop simulation of robots interacting with environment," 2002 IEEE International Conference on Robotics and Automation, vol. 1, pp. 523-529, IEEE, 2002.

[9] G. D. White, R. M. Bhatt, C. P. Tang, and V. N. Krovi, "Experimental evaluation of dynamic redundancy resolution in a nonholonomic wheeled mobile manipulator," *IEEE/ASME Transactions on Mechatronics*, vol. 14, no. 3, pp. 349-357, 2009.

[10] J. A. Buford, Jr., A. C. Jolly, S. B. Mobley, and W. J. Sholes, "Advancements in hardware-in-the-loop simulations at the U.S. Army aviation and missile command," SPIE - Technologies for Synthetic Environments: Hardware-in-the-Loop Testing V, R. L. Murrer (ed., vol. 4027, pp. 2-10, SPIE, 2000.

[11] E. G. Huber Jr and R. A. Courtney, "Hardware-in-the-loop simulation at wright laboratory's dynamic infrared missile evaluator (DIME) facility," 1997 Technologies for Synthetic Environments: Hardware-in-the-Loop Testing II, vol. 3084, pp. 2-8, SPIE, 1997.

[12] M. A. Kelf, "Hardware-in-the-loop simulation for undersea vehicle applications," SPIE - Technologies for Synthetic Environments: Hardware-in-the-Loop Testing VI, vol. 4366, pp. 1-12, SPIE, 2001.

[13] S. Mahin, R. Nigbor, C. Pancake, R. Reitherman, and S. Wood, "The establishment of the nees consortium," 2003 ASCE/SEI Structures Congress and Exposition: Engineering Smarter, pp. 181-182, American Society of Civil Engineers, 2003.

[14] E. Watanabe, T. Kitada, S. Kunitomo, and K. Nagata, "Parallel pseudodynamic seismic loading test on elevated bridge system through the internet," 8th East Asia-Pacific Conference on Structural Engineering and Construction, Singapore, 2001.

[15] K.-C. Tsai, C.-C. Yeh, Y.-S. Yang, K.-J. Wang, S.-J. Wang, and P.-C. Chen, "Seismic hazard mitigation: Internet-based hybrid testing framework and examples," International Colloquium on Natural Hazard Mitigation: Methods and Applications, France, 2003.

[16] B. F. Spencer, A. Elnashai, N. Nakata, H. Saliem, G. Yang, J. Futrelle, W. Glick, D. Marcusiu, K. Ricker, T. Finholt, D. Horn, P. Hubbard, K. Keahey, L. Liming, N. Zaluzec, L. Pearlman, and E. Stauffer, "The most experiment: Earthquake engineering on the grid," NEESgrid, Technical Report NEESgrid-2004-41, 2004.

[17] P. Pan, M. Tada, and M. Nakashima, "Online hybrid test by internet linkage of distributed test-analysis domains," *Earthquake Engineering and Structural Dynamics*, vol. 34, no. 11, pp. 1407-1425, 2005.

[18] B. Stojadinovic, G. Mosqueda, and S. A. Mahin, "Event-driven control system for geographically distributed hybrid simulation," *Journal of Structural Engineering*, vol. 132, no. 1, pp. 68-77, 2006.

[19] G. Mosqueda, B. Stojadinovic, J. Hanley, M. Sivaselvan, and A. M. Reinhorn, "Hybrid seismic response simulation on a geographically distributed bridge model," *Journal of Structural Engineering*, vol. 134, no. 4, pp. 535-543, 2008.

[20] M. Compere, J. Goodell, M. Simon, W. Smith, and M. Brudnak, "Robust control techniques enabling duty cycle experiments utilizing a 6-DOF crewstation motion base, a full scale combat hybrid electric power system, and long distance internet communications," *SAE Technical Paper,* 2006-01-3077, 2006.

[21] J. Goodell, M. Compere, M. Simon, W. Smith, R. Wright, and M. Brudnak, "Robust control techniques for state tracking in the presence of variable time delays," *SAE Technical Paper,* 2006-01-1163, 2006.

[22] M. Brudnak, M. Pozolo, V. Paul, S. Mohammad, W. Smith, M. Compere, J. Goodell, D. Holtz, T. Mortsfield, and A. Shvartsman, "Soldier/harware-in-the-loop simulation-based combat vehicle duty cycle measurement: Duty cycle experiment 2," Simulation Interoperability Workshop, Norfolk, VA, Simulation Interoperability Standards Organization (SISO), 2007.

[23] T. Ersal, M. Brudnak, A. Salvi, J. L. Stein, Z. Filipi, and H. K. Fathy, "Development and model-based transparency analysis of an internet-distributed hardware-in-the-loop simulation platform," *Mechatronics*, vol. 21, no. 1, pp. 22-29, 2011.

[24] T. Ersal, M. Brudnak, J. L. Stein, and H. K. Fathy, "Statistical transparency analysis in internet-distributed hardware-in-the-loop simulation," *IEEE/ASME Transactions on Mechatronics*, in press.

[25] G. Niemeyer and J.-J. E. Slotine, "Toward bilateral internet teleoperation," in *Beyond webcams: An introduction to online robots*: MIT Press, 2002, pp. 193-213.

[26] G. Niemeyer and J.-J. E. Slotine, "Stable adaptive teleoperation," *IEEE Journal of Oceanic Engineering*, vol. 16, no. 1, pp. 152-162, 1991.

[27] R. J. Anderson and M. W. Spong, "Bilateral control of teleoperators with time delay," *IEEE Transactions on Automatic Control*, vol. 34, no. 5, pp. 494-501, 1989.

[28] D. Lee and M. W. Spong, "Passive bilateral teleoperation with constant time delay," *IEEE Transactions on Robotics*, vol. 22, no. 2, pp. 269-281, 2006.

[29] N. Xi and T. J. Tarn, "Stability analysis of non-time referenced internet-based telerobotic systems," *Robotics and Autonomous Systems*, vol. 32, no. 2, pp. 173-178, 2000.

[30] I. Elhajj, X. Ning, F. Wai Keung, L. Yun-Hui, Y. Hasegawa, and T. Fukuda, "Supermedia-enhanced internet-based telerobotics," *Proceedings of the IEEE*, vol. 91, no. 3, pp. 396-421, 2003.

[31] D. A. Lawrence, "Stability and transparency in bilateral teleoperation," *IEEE Transactions on Robotics and Automation*, vol. 9, no. 5, pp. 624-637, 1993.

[32] M. C. Çavuşoğlu, A. Sherman, and F. Tendick, "Design of bilateral teleoperation controllers for haptic exploration and telemanipulation of soft environments," *IEEE Transactions on Robotics and Automation*, vol. 18, no. 4, pp. 641-647, 2002.

[33] G. De Gersem, H. Van Brussel, and F. Tendick, "Reliable and enhanced stiffness perception in soft-tissue telemanipulation," *International Journal of Robotics Research*, vol. 24, no. 10, pp. 805-822, 2005.

[34] Y. Yokokohji and T. Yoshikawa, "Bilateral control of master-slave manipulators for ideal kinesthetic coupling - formulation and experiment," *IEEE Transactions on Robotics and Automation*, vol. 10, no. 5, pp. 605-619, 1994.

[35] P. G. Griffiths, R. B. Gillespie, and J. S. Freudenberg, "A fundamental trade off between performance and sensitivity within haptic rendering," *IEEE Transactions on Robotics*, vol. 24, no. 3, pp. 537-548, 2008.

[36] J. S. Freudenberg, C. V. Hollot, R. H. Middleton, and V. Toochinda, "Fundamental design limitations of the general control configuration," *IEEE Transactions on Automatic Control*, vol. 48, no. 8, pp. 1355-1370, 2003.